Available online at www.sciencedirect.com
ScienceDirect
Journal of Organometallic Chemistry 692 (2007) 2193–2204
Journal of Organometallic Chemistry
www.elsevier.com/locate/jorganchem

Structural and spectroscopic trends in mononuclear arylchalcogenolato-palladium(II) and -platinum(II) complexes: Crystal structures of [M(TeAr)$_2$(dppe)] {M = palladium, platinum; Ar = phenyl, 2-thienyl; dppe = 1,2-bis(diphenylphosphino)ethane}

Maarit Risto, Esther M. Jahr, Milja S. Hannu-Kuure, Raija Oilunkaniemi *, Risto S. Laitinen *

Department of Chemistry, University of Oulu, P.O. Box 3000, FI-90014 Oulu, Finland

Received 15 December 2006; received in revised form 21 January 2007; accepted 22 January 2007
Available online 30 January 2007

Abstract

A series of mononuclear [M(EAr)$_2$(dppe)] [M = Pd, Pt; E = Se, Te; Ar = phenyl, 2-thienyl; dppe = 1,2-bis(diphenylphosphino)ethane] complexes has been prepared in good yields by the reactions of [MCl$_2$(dppe)] and corresponding ArE$^-$ with a special emphasis on the aryltellurolatopalladium and -platinum complexes for which the existing structural information is virtually non-existent. The complexes have crystallized in five isomorphic groups: (1) [Pd(SePh)$_2$(dppe)] and [Pt(SePh)$_2$(dppe)], (2) [Pd(TePh)$_2$(dppe)] and [Pt(TePh)$_2$(dppe)], (3) [Pd(SeTh)$_2$(dppe)], (4) [Pt(SeTh)$_2$(dppe)] and [Pd(TeTh)$_2$(dppe)], and (5) [Pt(TePh)$_2$(dppe)]. In addition, solvated [Pd(TePh)$_2$(dppe)] · CH$_3$OH and [Pd(TeTh)$_2$(dppe)] · 1/2CH$_2$Cl$_2$ could be isolated and structurally characterized. The metal atom in each complex exhibits an approximate square-planar coordination. The Pd–Se, Pt–Se, Pd–Te, and Pt–Te bonds span a range of 2.4350(7)–2.4828(7) Å, 2.442(1)–2.511(1) Å, 2.5871(7)–2.6704(8) Å, and 2.6053(6)–2.6594(9) Å, respectively, and the respective Pd–P and Pt–P bond distances are 2.265(2)–2.295(2) Å and 2.247(2)–2.270(2) Å. The orientation of the arylchalcogenolato ligands with respect to the M(E$_2$)(P$_2$) plane has been found to depend on the E–M–E bond angle. The NMR spectroscopic information indicates the formation of only *cis*-[M(EAr)$_2$(dppe)] complexes in solution. The trends in the ^{31}P, ^{77}Se, ^{125}Te, and ^{195}Pt chemical shifts expectedly depend on the nature of metal, chalcogen, and aryl group. Each trend can be considered independently of other factors. The ^{77}Se or ^{125}Te resonances appear as second-order multiplets in case of palladium and platinum complexes, respectively. Spectral simulation has yielded all relevant coupling constants.

Keywords: Organotellurium ligands; Organoselenium ligands; Palladium complexes; Platinum complexes; X-ray crystallography; NMR spectroscopy

1. Introduction

The role of chalcogenolato complexes of palladium and platinum in the Pd(0) and Pt(0) catalyzed reactions of Ar$_2$S$_2$ and Ar$_2$Se$_2$ with alkynes has recently been discussed [1–6]. In case of the Pd(0) catalyst, the S–S or Se–Se bond addition to alkynes involves a dinuclear palladium intermediate [Pd$_2$(EAr)$_4$L$_2$] (E = S, Se; L = phosphine or a related ligand) [1–6]. Such complexes have been isolated after the oxidative addition of Ar$_2$E$_2$ to [PdL$_4$] or substitution reaction of the chloride ligands in [PdCl$_2$L$_2$] by ArE$^-$ [7–10]. The reaction utilizing the Pt(0) catalyst seems to proceed with a different mechanism, since platinum does not show as good propensity for the formation of polynuclear complexes as palladium [2]. It has been suggested that

* Corresponding authors. Fax: +358 8 553 1608 (R.S. Laitinen).
E-mail address: Risto.Laitinen@oulu.fi (R.S. Laitinen).

0022-328X/$ - see front matter © 2007 Elsevier B.V. All rights reserved.
doi:10.1016/j.jorganchem.2007.01.039

mononuclear *cis*-[Pt(EAr)$_2$L$_2$] complexes are catalytically active, but the catalyst degrades with time because of the formation of the *trans*-isomer [2].

We have recently investigated the ligand substitution reactions of different arylselenolates with *trans*-[PdCl$_2$(PPh$_3$)$_2$] and *cis*-[PtCl$_2$(PPh$_3$)$_2$]. Whereas the reactions involving palladium afforded solely dinuclear [Pd$_2$(SeAr)$_4$(PPh$_3$)$_2$] [11–13], those involving *cis*-[PtCl$_2$(PPh$_3$)$_2$] initially produced *cis*-[Pt(SeAr)$_2$(PPh$_3$)$_2$] that subsequently underwent facile isomerization from *cis* to *trans* form in solution [14,15]. The DFT calculations of model [Pt(SeAr)$_2$(PH$_3$)$_2$] (Ar = Ph, 2-thienyl, 2-furyl) isomers indicated that the *cis*-isomers indeed lie at higher energy than the *trans*-isomers [15] providing a rationale for the *cis–trans* interconversion.

Similar product distributions and equally facile isomerization have been observed in the reactions of [Pd(PPh$_3$)$_4$] and [Pt(PPh$_3$)$_4$] with Ar$_2$Se$_2$ [2,7,16]. It has also been reported that the oxidative addition of Ar$_2$Te$_2$ to [Pd(PPh$_3$)$_2$] affords a dinuclear complex [17,18], though the reaction has also been shown to produce hexanuclear complexes [16].

Interestingly, the *cis–trans* isomerization of mononuclear selenolato complexes seems to be dependent on the electron-withdrawing power of the organic substituent bonded to selenium, since the related *cis*-[Pt(SeR)$_2$(PPh$_3$)$_2$] (R = ^{n}Bu, ^{t}Bu) do not seem to undergo isomerization [19], though the DFT calculations of model [Pt(SeR)$_2$(PH$_3$)$_2$] isomers indicate that the *cis*-isomers lie at higher relative energy than the *trans*-isomers even in the alkyselenolato complexes [15]. Evidently, the solvent also plays a role. Isomerization of *cis*-[Pt(SeCF$_3$)$_2$(PPh$_3$)$_2$] with electronegative trifluoromethylselenolato ligands to the *trans*-form takes place rapidly in dichloromethane, but the process in acetonitrile is much slower [20]. While the investigations of the analogous tellurolato complexes are sparse [20,21], it has been reported that, contrary to the analogous selenolato complex, there was no evidence of the isomerization of *cis*-[Pt(TeCF$_3$)$_2$(PPh$_3$)$_2$] to the *trans* form [20].

The formation of dinuclear palladium complexes is avoided by using a chelating phosphine ligand [22–25] and it also forces the formation of only the *cis*-isomer. It has been reported that [M(SAr)$_2$(dppe)] and [M(SeAr)$_2$(dppe)] [M = Pd, Pt; Ar = Ph; dppe = 1,2-bis(diphenylphosphino)ethane] are virtually catalytically inactive for the addition of Ar$_2$E$_2$ to alkynes [2], but it is an open question, whether the replacement of sulfur or selenium by tellurium would lead to improved catalytic properties of the complexes.

In order to further explore the chemistry of chalcogenolato complexes of palladium and platinum, we report here a study of the synthesis, NMR spectroscopic properties, and crystal structures of a series of [M(EAr)$_2$(dppe)] (M = Pd, Pt; E = Se, Te; Ar = Ph, 2-thienyl). While the preparations of [M(EPh)$_2$(dppe)] (M = Pd, Pt; E = Se, Te) have been reported previously {E = Se [22–24], Te [22]} the only crystal structure of the series determined to date is that of [Pd(SePh)$_2$(dppe)] · C$_6$H$_6$ [24].

2. Experimental

2.1. General

All reactions and manipulations of air- and moisture-sensitive reagents were carried out under an inert atmosphere by using a standard glovebox or Schlenk techniques. [PdCl$_2$(dppe)] (Aldrich), Ph$_2$Se$_2$ (Aldrich), Ph$_2$Te$_2$ (Aldrich), *n*-butyl lithium (2.5 M in hexanes, Aldrich), tellurium (Aldrich), and selenium (Merck) were used as supplied. [PtCl$_2$(dppe)] was prepared by the method of Appleton et al. [26]. Thiophene (Aldrich) was purified by distillation and purged with argon before use. Methanol was dried on molecular sieves and degassed with argon. Toluene and *n*-hexane were dried by distillation over Na/benzophenone and CH$_2$Cl$_2$ was dried over P$_4$O$_{10}$ under an argon atmosphere prior to use.

2.2. Synthesis of [M(EAr)$_2$(dppe)] (**1**)–(**8**)

2.2.1. [Pd(SePh)$_2$(dppe)] (**1**)

0.089 g (0.285 mmol) of Ph$_2$Se$_2$ in 5 ml of methanol was treated with NaBH$_4$ until the solution became transparent. The resulting solution was added to a suspension of 0.149 g (0.260 mmol) of [PdCl$_2$(dppe)] in 10 ml toluene. The reaction mixture was stirred overnight at room temperature. Volatile materials were removed under dynamic vacuum. The red solid residue was dissolved in dichloromethane (10 ml), filtered, and concentrated by partial evaporation of the solvent. [Pd(SePh)$_2$(dppe)] was precipitated by adding *n*-hexane into the solution. The orange solid product was filtered off, washed with hexane and dried. Isolated yield 0.131 g (62%). Anal. Calc. for C$_{38}$H$_{34}$P$_2$Se$_2$Pd: C, 55.86; H, 4.20. Found: C, 54.65; H, 4.30%.

Complexes **2**–**4** were prepared in a similar fashion to **1**.

2.2.2. [Pt(SePh)$_2$(dppe)] (**2**)

0.172 g (0.260 mmol) of [PtCl$_2$(dppe)] and 0.089 g (0.285 mmol) of Ph$_2$Se$_2$. Yield 0.130 g (55%). Yellow solid. Anal. Calc. for C$_{38}$H$_{34}$P$_2$Se$_2$Pt: C, 50.39; H, 3.78. Found: C, 50.11; H, 3.64%.

2.2.3. [Pd(TePh)$_2$(dppe)] (**3**)

0.251 g (0.436 mmol) [PdCl$_2$(dppe)] and 0.200 g (0.489 mmol) Ph$_2$Te$_2$. Yield 0.249 g (63%). Reddish brown solid. Anal. Calc. for C$_{38}$H$_{34}$P$_2$Te$_2$Pd: C, 49.92; H, 3.75. Found: C, 49.08; H 3.63%.

2.2.4. [Pt(TePh)$_2$(dppe)] (**4**)

0.131 g (0.197 mmol) [PtCl$_2$(dppe)] and 0.089 g (0.217 mmol) Ph$_2$Te$_2$. Stirred for 2 h. Yield 0.084 g (42%).

Orange solid. Anal. Calc. for $C_{38}H_{34}P_2Te_2Pt$: C, 45.50; H, 3.42. Found: C, 45.54; H 3.32%.

2.2.5. [Pd(SeTh)$_2$(dppe)] (**5**)

1.5 ml (3.75 mmol) *n*-BuLi was added to a solution of 0.33 ml (4.12 mmol) of thiophene in 8 ml of THF. Freshly ground selenium (0.281 g, 3.56 mmol) was added into the reaction solution after 30 min. The reaction mixture was stirred at room temperature for further 40 min. 4.00 ml of the resulting LiSeTh solution (1.45 mmol) was added to a solution of [$PdCl_2$(dppe)] (0.386 g, 0.67 mmol) in 15 ml of CH_2Cl_2. The reaction mixture was stirred for 2 h, filtered, and concentrated by a partial evaporation of the solvent. [Pd(SeTh)$_2$(dppe)] was precipitated by adding *n*-hexane into the solution. The orange product was filtered off, washed with *n*-hexane and dried. Yield 0.496 g (94%). Anal. Calc. for $C_{34}H_{30}P_2S_2Se_2Pd$: C, 46.02; H, 4.12; S, 8.19. Found: C, 46.23; H, 3.87; S, 7.40%.

Complexes **6**–**8** were prepared in a similar fashion to **5**.

2.2.6. [Pt(SeTh)$_2$(dppe)] (**6**)

0.153 g (0.230 mmol) [$PtCl_2$(dppe)] and 0.507 mmol LiSeTh. Yield 0.093 g (46%). Yellow solid. Anal. Calc. for $C_{38}H_{34}P_2Se_2Pt$: C, 44.50; H, 3.30; S, 6.99. Found: C, 43.63; H, 3.31; S, 7.16%.

2.2.7. [Pd(TeTh)$_2$(dppe)] (**7**)

0.249 g (0.432 mmol) [$PdCl_2$(dppe)] and 0.950 mmol LiTeTh. Stirred overnight. Yield 0.301 g (75%). Purple solid. Anal. Calc. for $C_{38}H_{34}P_2Te_2Pd$: C, 44.08; H, 3.26; S, 6.92. Found: C, 44.22; H, 3.31; S, 6.81%.

2.2.8. [Pt(TeTh)$_2$(dppe)] (**8**)

0.100 g (0.151 mmol) [$PtCl_2$(dppe)] and 0.331 mmol LiTeTh. Yield 0.070 g (46%). Orange solid. Anal. Calc. for $C_{38}H_{34}P_2Te_2Pt$: C, 40.23; H, 2.98; S, 6.32. Found: C, 39.76; H, 2.85; S, 6.33%.

2.3. NMR spectroscopy

The $^{31}P\{^1H\}$, ^{77}Se, ^{125}Te, and ^{195}Pt NMR spectra were recorded in CH_2Cl_2 on a Bruker DPX400 spectrometer operating at 161.98, 76.31, 126.29, and 85.57 MHz, respectively. The typical respective spectral widths were 48.543, 100.000, 100.000, and 85.47 kHz, and the respective pulse widths were 7.50, 6.70, 6.67, and 10.00 μs. The pulse delays were 1.0, 2.0, 1.5, and 0.01 s for ^{31}P, ^{77}Se, ^{125}Te, and ^{195}Pt, respectively. Orthophosphoric acid (85%), saturated solutions of SeO_2 (aq) and H_6TeO_6 (aq), and K_2PtCl_6 in D_2O were used as external standards. The ^{31}P and ^{195}Pt chemical shifts are reported relative to the external standards, and the ^{77}Se and ^{125}Te chemical shifts relative to neat Me_2Se

Table 1
Details of the crystal structure determination of complexes **1**–**4**

	1	**2**	**3**	**3 · CH$_3$OH**	**4**
Empirical formula	$C_{38}H_{34}P_2PdSe_2$	$C_{38}H_{34}P_2PtSe_2$	$C_{38}H_{34}P_2PdTe_2$	$C_{39}H_{38}OP_2PdTe_2$	$C_{38}H_{34}P_2PtTe_2$
Relative molecular mass	816.91	905.60	914.19	946.23	1002.88
Crystal system	Monoclinic	Monoclinic	Monoclinic	Monoclinic	Monoclinic
Space group	$P2_1/n$	$P2_1/n$	$P2_1/c$	$P2_1/n$	$P2_1/c$
a (Å)	17.943(4)	17.925(4)	10.451(2)	10.106(2)	10.480(2)
b (Å)	11.563(2)	11.535(2)	15.395(3)	16.058(3)	15.260(3)
c (Å)	32.161(6)	32.199(6)	21.736(4)	23.519(5)	21.753(4)
β (°)	95.06(3)	95.03(3)	96.19(3)	96.90(3)	96.30(3)
V (Å^3)	6647(2)	6632(2)	3477(1)	3789(1)	3458(1)
Z	8	8	4	4	4
F(000)	3248	3504	1768	1840	1896
D_{calc} (g cm^{-3})	1.633	1.814	1.747	1.659	1.926
μ (Mo Kα) (mm^{-1})	2.872	6.550	2.296	2.112	5.830
Crystal size (mm)	0.20 × 0.20 × 0.20	0.25 × 0.20 × 0.05	0.30 × 0.15 × 0.05	0.20 × 0.20 × 0.10	0.50 × 0.15 × 0.10
θ Range (°)	2.99–26.00	3.00–25.00	2.47–26.00	3.08–26.00	3.13–26.00
Number of reflections collected	49101	37481	20688	59149	50249
Number of unique reflections	12987	10836	6702	7411	6767
Number of observed reflections[a]	10247	9101	5199	6435	6304
Number of parameters	776	776	388	415	388
R_{int}	0.0811	0.0779	0.0692	0.1426	0.0699
R_1[b]	0.0445	0.0472	0.0480	0.0579	0.0343
wR_2 (all data)[b]	0.1101	0.1208	0.1389	0.1612	0.0922
Goodness-of-fit	1.028	1.013	1.171	1.108	1.055
Maximum and minimum heights in final difference Fourier synthesis (e Å^{-3})	0.906, −0.806	1.570, −1.736	0.936, −1.288	2.322, −1.982	2.139, −1.828

[a] $I \geqslant 2\sigma(I)$.
[b] $R_1 = \sum||F_o| - |F_c||/\sum|F_o|$, $wR_2 = [\sum w(F_o^2 - F_c^2)^2/\sum wF_o^4]^{1/2}$.

Table 2
Details of the crystal structure determination of complexes **5**–**8**

	5	**6**	**7**	**7** · 1/2CH_2Cl_2	**8**
Empirical formula	$C_{34}H_{30}P_2PdS_2Se_2$	$C_{34}H_{30}P_2PtS_2Se_2$	$C_{34}H_{30}P_2PdS_2Te_2$	$C_{34.50}H_{31}ClP_2PdS_2Te_2$	$C_{34}H_{30}P_2PtS_2Te_2$
Relative molecular mass	828.96	917.65	926.24	968.70	1014.93
Crystal system	Orthorhombic	Monoclinic	Monoclinic	Monoclinic	Monoclinic
Space group	$P2_12_12_1$	$P2_1$	$P2_1$	$P2_1/n$	$P2_1/c$
a (Å)	11.655(2)	9.542(2)	9.650 (29)	11.029(2)	11.926(2)
b (Å)	16.465(3)	16.990(3)	16.997(3)	20.924(4)	16.098(3)
c (Å)	17.156(3)	10.290(2)	10.567(2)	15.224(3)	17.080(3)
β (°)		108.61(3)	108.60(3)	93.63(3)	97.07(3)
V (Å^3)	3292(1)	1581.0(6)	1642.7(6)	3506 (1)	3254(1)
Z	4	2	2	4	4
F (000)	1640	884	892	1868	1912
D_{calc} (g cm^{-3})	1.672	1.928	1.873	1.835	2.072
μ (Mo Kα) (mm^{-1})	3.022	6.997	2.554	2.471	6.320
Crystal size (mm)	0.15 × 0.15 × 0.08	0.20 × 0.10 × 0.05	0.30 × 0.15 × 0.10	0.15 × 0.12 × 0.10	0.20 × 0.20 × 0.05
θ Range (°)	3.03–26.00	3.18–26.00	3.27–26.00	3.98–26.00	3.05–26.00
Number of reflections collected	17226	10810	24286	19593	27259
Number of unique reflections	6298	5309	5756	6613	6379
Number of observed reflections[a]	5597	4893	5756	4990	5349
Number of parameters	370	343	372	381	367
R_{int}	0.0800	0.0494	0.0639	0.1194	0.1327
R_1[b]	0.0474	0.0432	0.0413	0.0685	0.0557
wR_2 (all data)[b]	0.1340	0.1212	0.1043	0.2015	0.1407
Goodness-of-fit	1.093	1.099	1.012	1.022	1.056
Maximum and minimum heights in final difference Fourier synthesis (e Å^{-3})	0.643, −0.844	1.180, −1.236	0.732, −1.232	5.276, −2.518	1.970, −1.513

[a] $I \leqslant 2\sigma(I)$.
[b] $R_1 = \sum||F_o| - |F_c||/\sum|F_o|$, $wR_2 = [\sum w(F_o^2 - F_c^2)^2/\sum wF_o^4]^{1/2}$.

and Me_2Te, respectively [$\delta(Me_2Se) = \delta(SeO_2) + 1302.6$; $\delta(Me_2Te) = \delta(H_6TeO_6) + 712$]. All spectra were recorded unlocked.

The spectral simulations were carried out by using the program Isotopomer [27].

2.4. X-ray crystallography

Diffraction data for compounds **1**–**3**, **3** · CH_3OH, **4**–**7**, **7** · 1/2CH_2Cl_2, and **8** were collected on a Nonius Kappa CCD diffractometer at 120 K using graphite monochromated Mo Kα radiation ($\lambda = 0.71073$ Å). Crystal data and details of the structure determinations are given in Tables 1 and 2. The X-ray quality crystals of **1**–**4** and **6**–**8** were obtained by crystallization from CH_2Cl_2 layered with *n*-hexane. **3** · CH_3OH was isolated upon recrystallization of the crude product from toluene. The X-ray-quality crystals of **5** and **7** · 1/2CH_2Cl_2 were obtained from CH_2Cl_2 by slow evaporation of the solvent.

All structures were solved by direct methods using SIR-92 [28] and refined using SHELXL-97 [29]. After the full-matrix least-squares refinement of non-hydrogen atoms with anisotropic thermal parameters, the hydrogen atoms were placed in calculated positions in the aromatic rings (C–H = 0.95 Å) and in the methyl and methylene groups (C–H = 0.99). In the final refinement the hydrogen atoms were riding with the carbon atom they were bonded to. The isotropic thermal parameters of the aromatic hydrogen atoms were fixed at 1.2 times and the methyl and methylene hydrogen atoms were fixed at 1.5 times to that of the corresponding carbon atom. The scattering factors for the neutral atoms were those incorporated with the programs.

The thienyl groups in **6**–**8** and the solvent molecules in **3** · CH_3OH and **7** · 1/2CH_2Cl_2 turned out to be disordered. In the refinement the disorder was taken into account, and the site occupation factors of each disordered pair were refined by constraining their sums to unity. Since the site occupation factors and thermal parameters of the disordered atoms correlate with each other, the thermal parameters of the corresponding pairs of atoms were restrained to be equal.

3. Results and discussion

3.1. General

[M(EAr)$_2$(dppe)] (M = Pd, Pt; E = Se, Te; Ar = phenyl, 2-thienyl) were synthesized by the reaction of [MCl_2(dppe)] with NaEPh or LiETh using a slight excess of the chalcogenolate. All complexes were analyzed by NMR spectroscopy

and structurally characterized in the solid state by single crystal X-ray diffraction. All selenolato complexes are stable in air. Organyltellurolato palladium complexes, however, turned out to be moisture-sensitive and had to be manipulated under a dry, inert atmosphere. The decomposition of platinum complexes in the same conditions was not observed.

3.2. NMR spectroscopy

The $^{31}P\{^1H\}$, ^{77}Se, ^{125}Te, and ^{195}Pt NMR spectroscopic data of **1**–**8** are shown in Table 3. A single resonance in the $^{31}P\{^1H\}$ spectra of all complexes expectedly indicates that the reactions produce only *cis*-[M(EAr$_2$)(dppe)]. The chemical shifts and $^1J_{Pt-P}$ coupling constants (where applicable) are in agreement with those reported previously for [Pd(SePh)$_2$(dppe)] and [Pt(SePh)$_2$(dppe)] (in C_6D_6 [24]; in $CDCl_3$ [22,23]), as well as for [Pd(TePh)$_2$(dppe)] and [Pt(TePh)$_2$(dppe)] (in $CDCl_3$ [24]).

^{195}Pt chemical shifts shown in Table 3 are consistent with those of related [Pt(ER)$_2$(dppe)] complexes {ER = SePh (−4975 ppm [24]); $SeCH_2Ph$ (−4917 ppm [25]); $SeCH_2CH_2NMe_2$ (−4958 ppm [30]); Te(3-MeC_5H_3N) (−5311 ppm [31]); Te(4-EtOC_6H_4) (−5310 ppm [24])}. The ^{195}Pt chemical shifts and $^1J_{Pt-P}$ coupling constants of related complexes *cis*-[Pt(SePh)$_2$(PPh$_3$)$_2$], *cis*-[Pt(SeTh)$_2$(PPh$_3$)$_2$], *cis*-[Pt(Se^{t}Bu)$_2$(PPh$_3$)$_2$], and *cis*-[Pt(Se^{n}Bu)$_2$(PPh$_3$)$_2$] are −4904 ppm (2968 Hz) [15], −4863 ppm (3041 Hz) [15], −4772 ppm (2928 Hz) [19], and −4914 ppm (2935 Hz) [19], respectively.

The ^{77}Se and ^{125}Te NMR spectra of **1**–**8** exhibit single resonances that appear as second-order multiplets due to coupling to two chemically equivalent but magnetically inequivalent phosphorus nuclei. In the case of the platinum complexes, ^{195}Pt satellites are also observed. They are exemplified in Fig. 1 by comparison of the observed and calculated ^{125}Te resonances of the tellurolato complexes **3**, **4**, **7**, and **8**. The spectral simulations reproduce the observed coupling patterns well. The intensity distributions and the frequency separations of the multiplet components are symmetric with respect to the assignment of the two $^2J_{P-Te}$ constants of different magnitudes either to *cis*- or *trans*-coupling, and we cannot therefore assign unambiguously the $^2J_{P-Te}$ or $^2J_{P-Se}$ coupling constants. However, it has been deduced for related systems that the coupling is larger to a phosphorus in *trans*-position and smaller to the *cis*-phosphorus [32,33].

The ^{77}Se NMR spectroscopic data of **1**, **2**, **5**, and **6** are similar to those of [Pt(SePh)$_2$(dppe)] (251 ppm; $^2J_{Se-P}$ = 74 Hz, 11 Hz) and [Pd(SePh)$_2$(dppe)] (202 ppm; $^2J_{Se-P}$ = 80 Hz) [24]. The ^{77}Se chemical shifts of *cis*-[Pt(SePh)$_2$(PPh$_3$)$_2$], *cis*-[Pt(SeTh)$_2$(PPh$_3$)$_2$], *cis*-[Pt(Se^{t}Bu)$_2$(PPh$_3$)$_2$], and *cis*-[Pt(Se^{n}Bu)$_2$(PPh$_3$)$_2$] are 299 ppm [15], 187 ppm [15], 254 ppm [19], and 136 ppm [19], respectively.

No ^{125}Te NMR spectroscopic data have previously been reported for the tellurolato complexes of palladium and platinum. The closest comparison can be made by considering *trans* − [M(TeCOR)$_2$(PR$'_3$)$_2$] (M = Pd, Pt) [34]. The ^{125}Te chemical shifts in the Pd complexes span a range of 362.1–443.8 ppm and those in the Pt complexes 329.4–

Table 3
$^{31}P\{^1H\}$, ^{77}Se, ^{125}Te, and ^{195}Pt NMR data (δ in ppm) for complexes **1**–**8**

Compound	$^{31}P\{^1H\}$ (δ)[a,b]		^{77}Se (δ)[c]		^{125}Te (δ)[c]		^{195}Pt (δ)	
[Pd(SePh)$_2$(dppe)] (**1**)	53.5		248	$^2J_{P-Se}$ 77 Hz, 7 Hz $^2J_{P-P'}$ 14 Hz	–		–	
[Pt(SePh)$_2$(dppe)] (**2**)	47.1	$^1J_{Pt-P}$ 2951 Hz $^2J_{Se-P}$ 70 Hz	204	$^1J_{Pt-Se}$ 186 Hz $^2J_{P-Se}$ 77 Hz, −14 Hz $^2J_{P-P'}$ = 10 Hz	–		−4960	$^1J_{Pt-P}$ 2951 Hz
[Pd(TePh)$_2$(dppe)] (**3**)	48.2		–		297	$^2J_{P-Te}$ 149 Hz, 38 Hz $^2J_{P-P'}$ 30 Hz	–	
[Pt(TePh)$_2$(dppe)] (**4**)	46.8	$^1J_{Pt-P}$ 2896 Hz $^2J_{Te-P}$ 126 Hz	–		177	$^1J_{Pt-Te}$ 902 Hz $^2J_{P-Te}$ 130 Hz, 43 Hz $^2J_{P-P'}$ 10 Hz	−5313	$^1J_{Pt-P}$ 2890 Hz
[Pd(SeTh)$_2$(dppe)] (**5**)	54.5		163	$^2J_{P-Se}$ 63, 15 Hz $^2J_{P-P'}$ 10 Hz	–		–	
[Pt(SeTh)$_2$(dppe)] (**6**)	47.6	$^1J_{Pt-P}$ 3002 Hz $^2J_{Se-P}$ 61 Hz	107	$^1J_{Pt-Se}$ 216 Hz $^2J_{P-Se}$ 65 Hz, 15 Hz $^2J_{P-P'}$ = 10 Hz	–		−4947	$^1J_{Pt-P}$ 3006 Hz
[Pd(TeTh)$_2$(dppe)] (**7**)	48.6		–		167	$^2J_{P-Te}$ 88, 64 Hz $^2J_{P-P'}$ 10 Hz	–	
[Pt(TeTh)$_2$(dppe)] (**8**)	47.2	$^1J_{Pt-P}$ 2907 Hz $^2J_{Te-P}$ 94 Hz	–		45	$^1J_{Pt-Te}$ 1036 Hz $^2J_{P-Te}$ 96 Hz, 58 Hz $^2J_{P-P'}$ 20 Hz	−5262	$^1J_{Pt-P}$ 2901 Hz

[a] The satellites due to the smaller of the two $^2J_{E-P}$ coupling constants are obscured by the main signal.

[b] The chalcogen satellites in the ^{31}P spectra of the palladium complexes **1**, **3**, **5**, and **7** only appear as shoulders at the side of the main resonance. While the $^2J_{P-E}$ coupling seems to be of the same order of magnitude as those deduced for the larger coupling from the simulations of the chalcogen resonances, it is not possible to estimate exact coupling constants.

[c] The coupling constants have been obtained from the simulations of the second-order ^{77}Se or ^{125}Te multiplets.

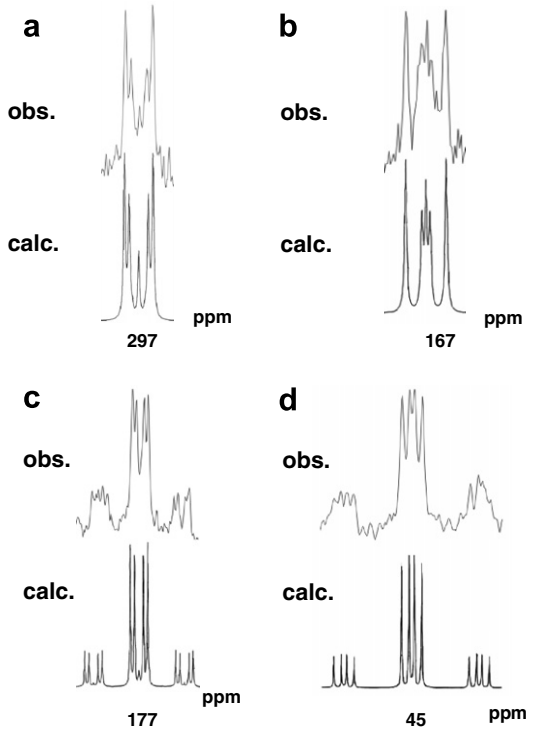

Fig. 1. The observed and simulated ^{125}Te resonances in (a) [Pd(TePh)$_2$(dppe)], (b) [Pd(TeTh)$_2$(dppe)], (c) [Pt(TePh)$_2$(dppe)], and (d) [Pt(TeTh)$_2$(dppe)]. The simulations yielded the following coupling constants: $^2J_{P-P'} = 30$ Hz [Pd(TePh)$_2$(dppe)], 10 Hz [Pd(TeTh)$_2$(dppe)], 10 Hz [Pt(TePh)$_2$(dppe)], and 20 Hz [Pt(TeTh)$_2$(dppe)]. For other relevant coupling constants, see Table 3.

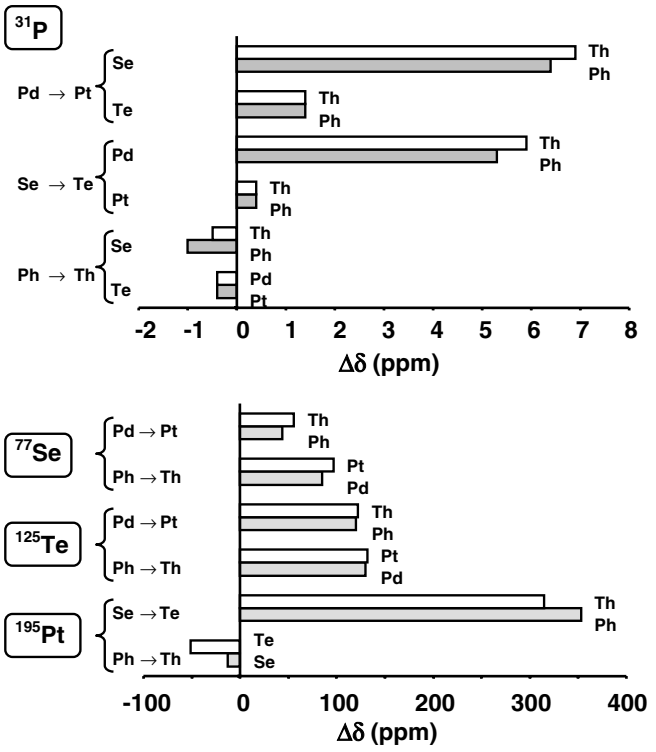

Fig. 2. The effect of varying the metal center (M = Pd, Pt), chalcogen atom (E = Se, Te), and the aryl group (Ar = Ph, Th) on the ^{31}P, ^{77}Se, ^{125}Te, and ^{195}Pt chemical shifts in [M(EAr)$_2$(dppe)] [dppe = 1,2-bis(diphenylphosphino)ethane].

532.2 ppm ($^1J_{Pt-Te}$: 681–812 Hz) [34]. These values, however, involve *trans*-isomers and only approximate agreement should be expected with *cis*-isomers of **3**, **4**, **7**, and **8**. The ^{77}Se resonances of the *cis*-isomers of various selenolato platinum complexes are found upfield from those of the *trans*-isomers. The $^1J_{Se-Pt}$ coupling constants of the *cis*-isomers are larger than those of the *trans*-isomers, These trends are exemplified by *cis*- and *trans*-[Pt(SePh)$_2$(PPh$_3$)$_2$] (299 and 176 ppm, respectively) [15]. The $^2J_{P-Te}$ coupling constants of **3**, **4**, **7**, and **8** can be compared with that of [PtCl{Te(C$_6$H$_4$OCH$_2$CH$_3$-4)}(PPh$_3$)$_2$] [35].

The trends in the chemical shifts are shown in Fig. 2. It is interesting to note that the relative changes in the chemical shifts when varying the metal, chalcogen, or the organic substituent in the complexes seem to be independent on changes in other parts of the molecule. For instance, the difference in the ^{31}P chemical shifts is 6.4 ppm between [Pd(SePh)$_2$(dppe)] and [Pt(SePh)$_2$(dppe)], and 6.9 ppm between [Pd(SeTh)$_2$(dppe)] and [Pt(SeTh)$_2$-(dppe)] with the resonance of the platinum complex appearing upfield. Similarly, the difference in the ^{125}Te chemical shifts is 120 ppm between [Pd(TePh)$_2$(dppe)] and [Pt(TePh)$_2$(dppe)], and 122 ppm between [Pd(TeTh)$_2$ (dppe)] and [Pt(TeTh)$_2$(dppe)] with the ^{125}Te resonance of the platinum complex appearing upfield in both cases. It can be seen from Fig. 2 that other chemical shifts behave in a similar fashion.

It has been known for a long time that many analogous tellurium and selenium compounds show a constant ratio of *ca.* 1.6 in the ^{125}Te and ^{77}Se chemical shifts [36]. While in the case of the Pt(II) and Pd(II) complexes, the analogous telluroether and selenoether complexes also show a similar ratio of 1.8 [37,38], it is interesting to note that in the case of current dppe complexes **1**–**8**, the $\delta(^{125}\text{Te}):\delta(^{77}\text{Se})$ ratios between the analogous species are significantly smaller. It can be seen from Table 3 that the $\delta(^{125}\text{Te}):\delta(^{77}\text{Se})$ ratio is 1.2 for **3** and **1** and 1.0 for **7** and **5**. Even smaller ratios of 0.9 and 0.4 are observed for the two pairs of platinum complexes **4**–**2** and **8**–**6**, respectively. The $\delta(^{125}\text{Te}):\delta(^{77}\text{Se})$ ratio for the tellurocarboxylato and selenocarboxylato *trans* – [M(ECOR)$_2$(PR$'_3$)$_2$] (M = Pt, Pd; E = Te, Se) is of the same order of magnitude (*ca.* 1.1–1.2) [34,39].

3.3. Crystal structures

The chalcogenolato complexes **1**–**8** can be subdivided into five isomorphic series: [Pd(SePh)$_2$(dppe)] (**1**) and [Pt(SePh)$_2$(dppe)] (**2**), [Pd(TePh)$_2$(dppe)] **(3)** and [Pt(TePh)$_2$-(dppe)] (**4**), [Pd(SeTh)$_2$(dppe)] (**5**), [Pt(SeTh)$_2$(dppe)] (**6**) and [Pd(TeTh)$_2$(dppe)] (**7**), and [Pt(TeTh)$_2$(dppe)] (**8**). Their molecular structures indicating the numbering of atoms are shown in Figs. 3–5. In addition, two complexes

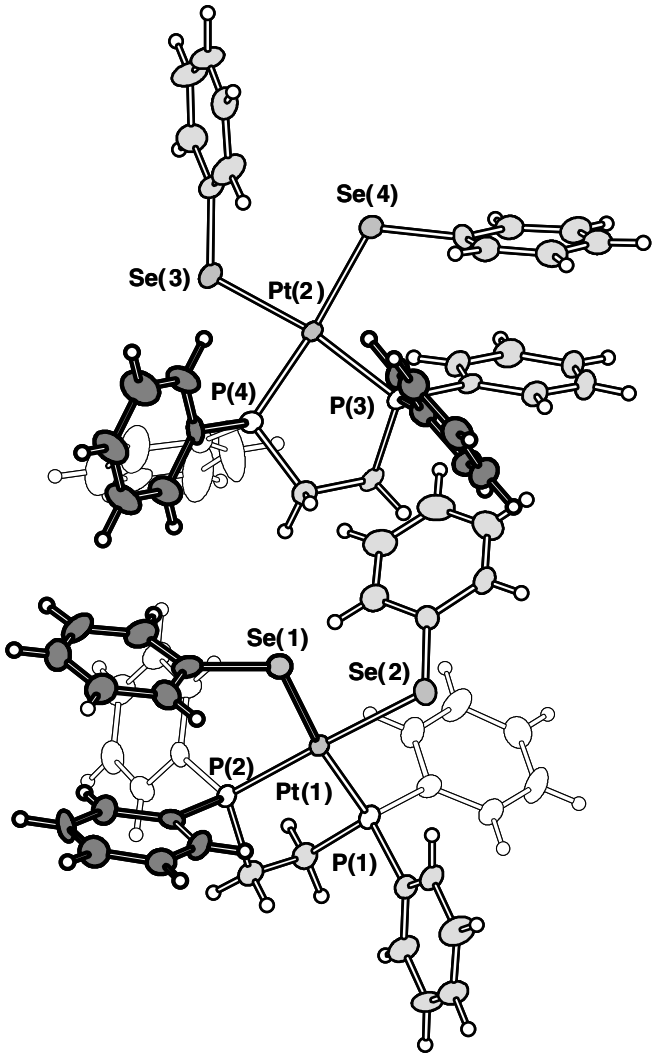

Fig. 3. The molecular structure of isomorphic [M(SePh)$_2$(dppe)] [M = Pd (**1**), Pt (**2**)] indicating the numbering of atoms. The thermal ellipsoids have been drawn at 50% probability level. The structure in the figure is that of **2**.

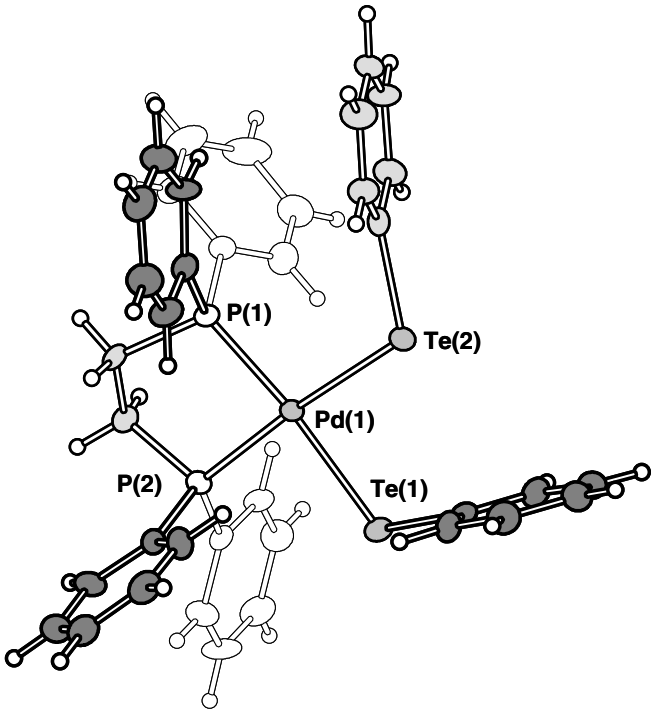

Fig. 4. The molecular structure of isomorphic [M(TePh$_2$)(dppe)] [M = Pd (**3**), Pt (**4**)] complex indicating the numbering of atoms. The thermal ellipsoids have been drawn at 50% probability level. The structure in the figure is that of **3**.

crystallize also with the solvent of crystallization: [Pd(TePh)$_2$(dppe)] · CH_3OH (**3** · CH_3OH) and [Pd(TeTh)$_2$-(dppe)] · 1/2CH_2Cl_2 (**7** · 1/2CH_2Cl_2). Their crystal structures indicating the numbering of atoms as well as the interaction with the disordered solvent molecules are shown in Fig. 6. Selected bond parameters of **1**–**4** are shown in Table 4 and those of **5**–**8** are shown in Table 5.

The lattice of each complex is composed of discrete molecular units with the metal atom exhibiting an approximate square-planar coordination [Σ_M = 359.97–360.52° (M = Pd, Pt)], though the individual bond angles are significantly deviated from the ideal value of 90°.

As shown in Tables 4 and 5, the Pd–Se bonds in **1** and **5** span a range of 2.4350(7)–2.4828(7) Å, and the Pt–Se bond lengths in **2** and **6** are 2.442(1)–2.511(1) Å. All these bonds correspond to single bond lengths and are in agreement with the Pd–Se bond lengths in [Pd(SePh)$_2$(dppe)] · C_6H_6 [2.444(1), 2.480(1) Å] [24], [Pd(SeCN)$_2$(dppe)] [2.478(1), 2.476(1) Å] [40], *trans*-[Pd(SePh)$_2$(P^{n}Bu$_3$)$_2$] [2.4609(4) Å] [41] and *trans*-[Pd(4-MeC$_6$H$_4$COSe)$_2$(PEt$_3$)$_2$] [2.456(1) Å] [39], as well as with the Pt–Se bond lengths in [Pt(SePh)$_2$(dppm)] [dppm = bis(diphenylphosphino)methane] [2.4340(9), 2.461(1) Å] [42], [Pt(SeCOPh)$_2$(dppp)] [dppp = 1,3-bis(diphenylphosphino)propane] [2.48218(11), 2.4613(10) Å] [43], and 2.4506(5)–2.5119(9) Å in *cis*- and *trans*-[Pt(SeAr)$_2$(PPh$_3$)$_2$] {Ar = Fu (2-furyl, C_4H_3O), Th (2-thienyl, C_4H_3S), Ph} [15].

The Pd–Te bond lengths in corresponding tellurolato complexes show a range of 2.5871(7)–2.6704(8) Å in **3**, **3** · CH_3OH, **7**, and **7** · 1/2CH_2Cl_2. They are consistent with the Pd–Te bond length of 2.6380(8) Å of the terminal thienyl tellurolato ligand in hexanuclear [Pd$_6$(Te$_4$)(TeTh)$_4$-(PPh$_3$)$_6$] [16], but they are slightly longer than those in [PdCl{Te(3-MeC$_5$H$_3$N)}(PPh$_3$)] [2.5606(8) Å] [31], [PdCl-(TeCH$_2$CH$_2$NMe$_2$)(P^{n}Pr$_3$)] [2.5095(8) Å], and [PdCl-(TeCH$_2$CH$_2$NMe$_2$)(PMePh$_2$)] [2.5161(6) Å] [44]. It reflects the stronger *trans*-influence of phosphorus compared to that of chlorine.

The Pt–Te bonds in **4** and **8** show the length range of 2.6053(6)–2.6594(9) Å. The bonds are in agreement with those of *cis*-[Pt(1,2-Te$_2$C$_6$H$_4$)(PPh$_3$)$_2$] [2.586(1) Å] [45], *trans*-[Pt(4-MeC$_6$H$_4$COTe)$_2$(PEt$_3$)$_2$] [2.592(1) and 2.632(2) Å] [34], and *cis*-[PtCl{Te(2,4,6-^{t}Bu$_3$C$_6$H$_2$)}-(PPh$_3$)$_2$] [2.614(1) Å] [46].

The respective Pd–P and Pt–P bond distances of 2.265(2)–2.295(2) Å and 2.247(2)–2.270(2) Å are quite normal for phosphine–metal coordination. They agree well

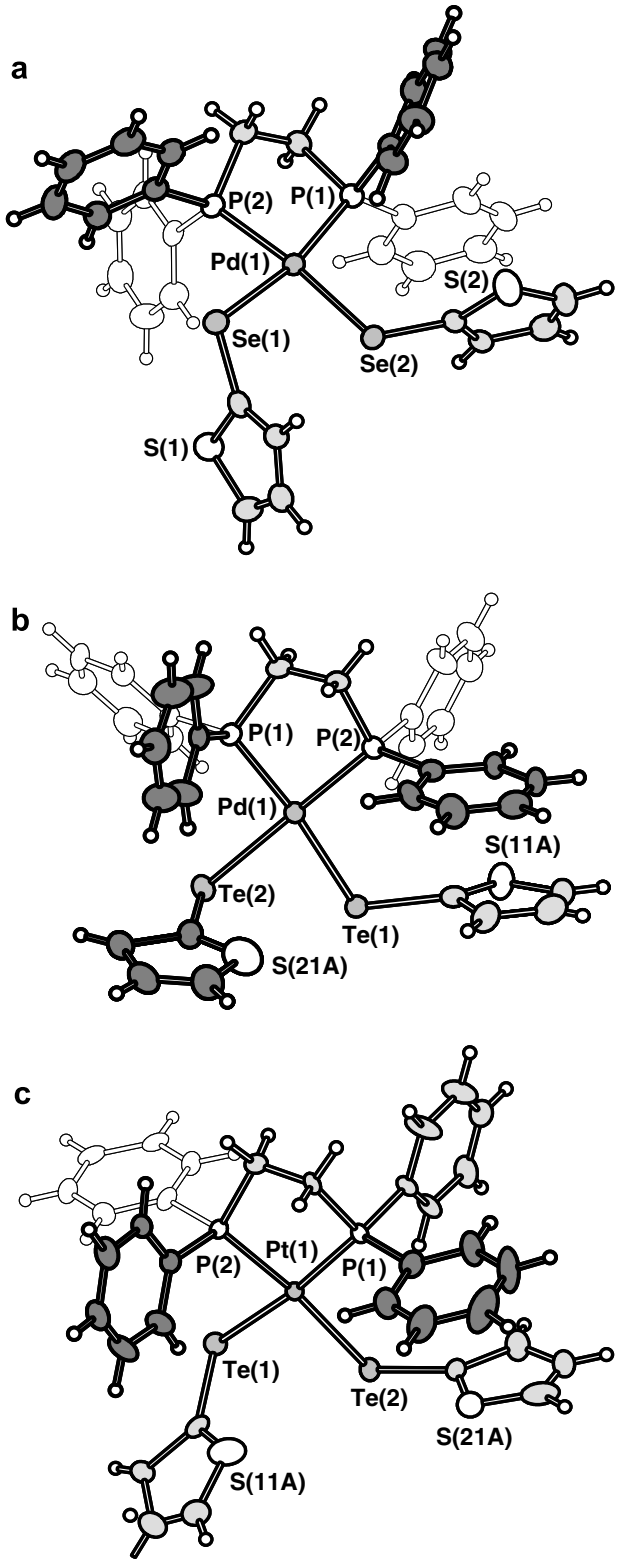

Fig. 5. The molecular structures of (a) [Pd(SeTh)$_2$(dppe)] (**5**), (b) isomorphic [Pt(SeTh)$_2$(dppe)] (**6**) and [Pd(TeTh)$_2$(dppe)] (**7**), and (c) [Pt(TeTh)$_2$(dppe)] (**8**) indicating the numbering of atoms. The thermal ellipsoids have been drawn at 50% probability level.

with those in [Pt_3Te_2(Th)(PPh_3)$_5$]Cl [2.266(7)–2.296(7) Å] [16] and [Pd_2(μ_2-Te)$_2$(dppe)$_2$] [2.286(2) and 2.287(2) Å] [47], but are slightly longer than those in [PdCl{Te(3-MeC_5H_3N)}(PPh_3)] [2.242(2) Å] [31], [PdCl($TeCH_2CH_2NMe_2$)(P^nPr_3)] [2.209(1) Å] [44] and [PdCl($TeCH_2CH_2NMe_2$)($PMePh_2$)] [2.230(1) Å] [44].

It is interesting to note that in each complex **1**–**8**, one of the E–M–E–C(aryl) torsional angles shows a range of 169.0(2)–179.9(3)° (see Tables 4 and 5). Therefore, the E–C(aryl) bond of one of the chalcogenolato ligands lies approximately on the square-planar M(E_2)(P_2) coordination plane with that of the other chalcogenolato ligand deviating from coplanarity. The angles between the relevant least-squares planes are shown in Fig. 7. The angle between the E–C(aryl) bond of the second chalcogenolato ligand and the M(E_2)(P_2) coordination plane is dependent on the E–M–E bond angle. When the bond angle is small, the E–C bond is approximately perpendicular to the coordination plane, but as the bond angle increases, also this E–C bond approaches coplanarity.

A second trend can also be seen from Fig. 7. When the E–C(aryl) bond is coplanar with the M(E_2)(P_2) plane, the corresponding M–E bond of the M–E–Ar moiety is approximately perpendicular to the plane of the aromatic ring. When the angle between the E–C bond and the M(E_2)(P_2) coordination plane is larger, the angle between the M–E bond and the plane of the aromatic ring decreases. When the E–C bond is perpendicular to the coordination plane, the M–E bond is almost coplanar with the aromatic ring. It has previously been observed that there are two possible stable conformations in diaryldiarylditellurides ArEEAr: one in which the E–E bond is perpendicular to both aromatic rings, and the other in which the aromatic rings are coplanar with the E–E bonds [48].

4. Conclusions

A series of mononuclear [M($EAr)_2$(dppe)] [M = Pd, Pt; E = Se, Te; Ar = phenyl, 2-thienyl; dppe = 1,2-bis(diphenylphosphino)ethane] complexes has been prepared in good yields by the reactions of [MCl_2(dppe)] with ArE^-. The trends in the structural and NMR spectroscopic properties of the complexes have been explored as a function of the identity of the metal center, chalcogen atom, and aromatic ring. In particular, we report in this contribution crystal structures of a number of aryltellurolato-palladium and -platinum complexes for which the existing solid state structural information is virtually non-existent.

The use of a chelating ligand forces the formation of mononuclear *cis*-chalcogenolato complexes. Those that have been prepared in this work crystallize in five isomorphic groups: (1) [Pd($SePh)_2$(dppe)] and [Pt($SePh)_2$(dppe)], (2) [Pd($TePh)_2$(dppe)] and [Pt($TePh)_2$(dppe)], (3) [Pd($SeTh)_2$(dppe)], (4) [Pt($SeTh)_2$(dppe)] and [Pd($TeTh)_2$(dppe)], and (5) [Pt($TePh)_2$(dppe)]. In addition, solvated [Pd($TePh)_2$(dppe)] · CH_3OH and [Pd($TeTh)_2$(dppe)] · 1/2CH_2Cl_2 could be isolated and structurally characterized.

The arylchalcogenolato ligands assume varying orientations with respect to the square-planar coordination sphere around the metal center. The chalcogen–carbon bond of

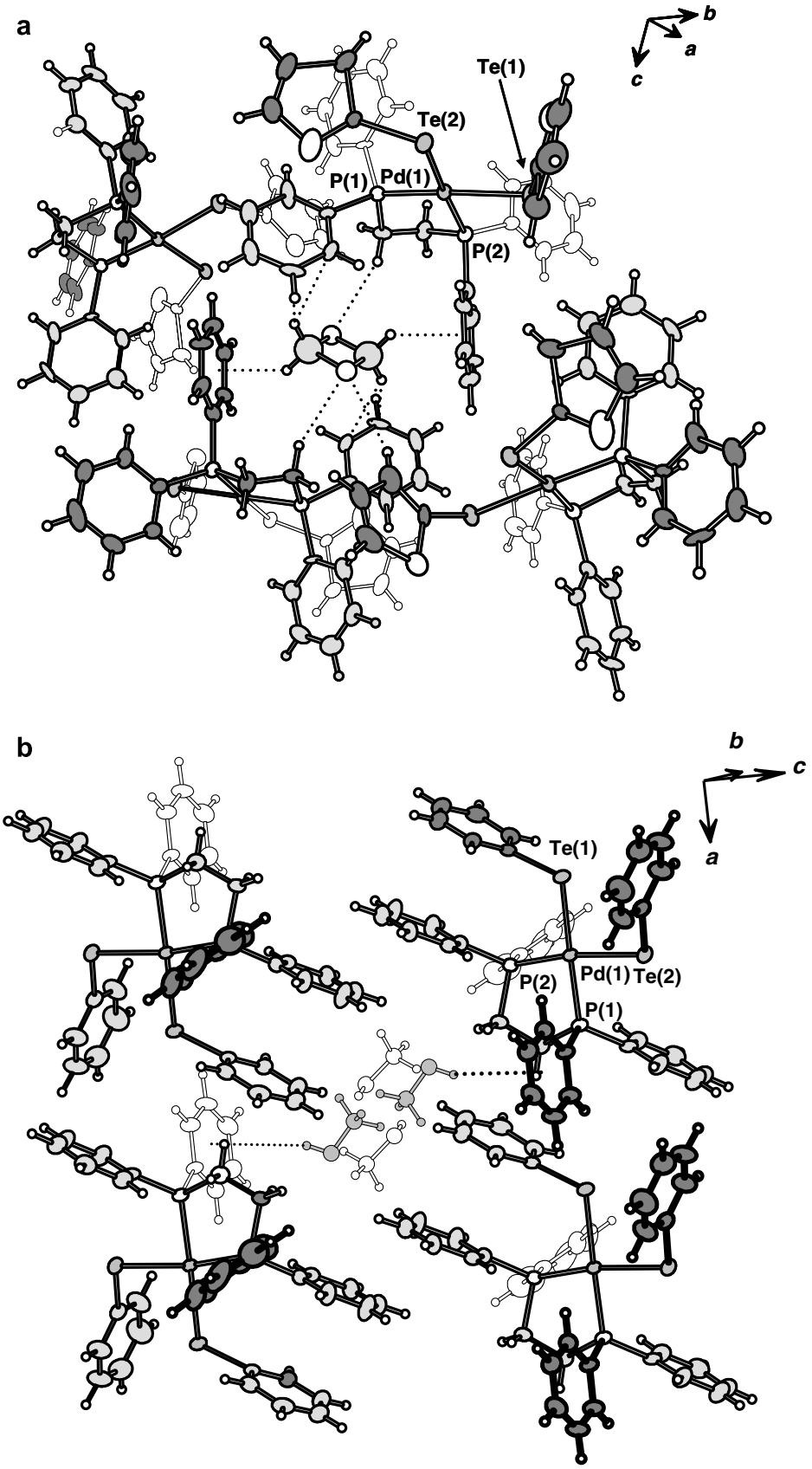

Fig. 6. The molecular structures of (a) $[Pd(TeTh)_2(dppe)] \cdot 1/2CH_2Cl_2$ ($\mathbf{7} \cdot 1/2CH_2Cl_2$) and (b) $[Pd(TePh)_2(dppe)] \cdot CH_3OH$ ($\mathbf{3} \cdot CH_3OH$) indicating the numbering of atoms. In both complexes the solvent is disordered (s.o.f. 0.5). The close contacts between the disordered solvent molecules and the complexes are also indicated in the figures. The thermal ellipsoids have been drawn at 50% probability level.

Table 4
Selected bond lengths (Å) and angles (°) of complexes **1**–**4**

	1	**2**	**3**	**3** · CH_3OH	**4**
M(1)–E(1)/M(2)–E(3)	2.4350(7)/2.4655(7)	2.442(1)/2.474(1)	2.6361(9)	2.5871(7)	2.6465(7)
M(1)–E(2)/M(2)–E(4)	2.4828(7)/2.4522(8)	2.492(1)/2.459(1)	2.5933(8)	2.6328(8)	2.6053(6)
M(1)–P(1)/M(2)–P(3)	2.274(1)/2.270(1)	2.252(2)/2.254(2)	2.279(2)	2.274(2)	2.251(1)
M(1)–P(2)/M(2)–P(4)	2.265(1)/2.277(1)	2.247(2)/2.250(2)	2.271(2)	2.278(2)	2.249(1)
E(1)–M(1)–E(2)	82.46(3)	81.59(4)	89.97(4)	89.42(3)	89.32(3)
E(1)–M(1)–P(1)	173.05(3)	172.24(6)	171.58(5)	172.06(4)	172.03(3)
E(1)–M(1)–P(2)	100.43(4)	101.08(6)	86.15(6)	99.83(5)	86.44(4)
E(2)–M(1)–P(1)	91.27(4)	91.34(6)	97.88(6)	85.87(5)	97.90(4)
E(2)–M(1)–P(2)	177.11(3)	177.28(6)	175.08(5)	169.74(4)	174.77(3)
P(1)–M(1)–P(2)	85.85(5)	86.02(8)	86.16(7)	85.40(6)	86.52(5)
E(3)–M(2)–E(4)	91.97(2)	90.76(3)			
E(3)–M(2)–P(3)	166.71(3)	167.40(6)			
E(3)–M(2)–P(4)	84.88(4)	85.37(6)			
E(4)–M(2)–P(3)	98.09(3)	98.39(6)			
E(4)–M(2)–P(4)	174.07(3)	174.38(6)			
P(3)–M(2)–P(4)	85.82(4)	86.06(7)			
E(2)–M(1)–E(1)–C(11)	−179.3(2)	−179.7(3)	22.6(2)	−169.8(2)	21.7(1)
E(1)–M(1)–E(2)–C(21)	−86.6(1)	−85.4(2)	169.0(2)	−21.6(2)	169.2(2)
E(4)–M(2)–E(3)–C(31)	−24.9(2)	−26.2(3)			
E(3)–M(2)–E(4)–C(41)	−175.9(2)	−177.5(3)			
M(1)–E(1)–C(11)–C(12)	−86.5(4)	−84.7(8)	−105.7(5)	−106.3(5)	−106.7(4)
M(1)–E(1)–C(11)–C(16)	102.9(3)	103.2(7)	75.7(6)	83.0(5)	75.1(4)
M(1)–E(2)–C(21)–C(22)	−173.4(4)	−174.1(6)	−83.0(6)	−76.9(5)	−81.9(4)
M(1)–E(2)–C(21)–C(26)	9.5(4)	8.2(7)	107.4(6)	106.0(6)	107.7(4)
M(2)–E(3)–C(31)–C(32)	−49.2(4)	−48.6(8)			
M(2)–E(3)–C(31)–C(36)	134.6(4)	134.4(6)			
M(2)–E(4)–C(41)–C(42)	−77.4(4)	−75.7(8)			
M(2)–E(4)–C(41)–C(46)	107.9(3)	109.0(6)			

Table 5
Selected bond lengths (Å) and angles (°) of complexes **5**–**8**

	5	**6**	**7**	**7** · 1/2 CH_2Cl_2	**8**
M(1)–E(1)	2.480(1)	2.451(1)	2.5871(8)	2.619(1)	2.6594(9)
M(1)–E(2)	2.455(1)	2.511(1)	2.6704(8)	2.609(1)	2.607(1)
M(1)–P(1)	2.274(2)	2.263(2)	2.292(2)	2.292(3)	2.267(2)
M(1)–P(2)	2.265(2)	2.270(2)	2.295(2)	2.283(3)	2.257(2)
E(1)–M(1)–E(2)	90.15(3)	80.88(5)	79.56(4)	89.71(3)	82.09(3)
E(1)–M(1)–P(1)	168.30(6)	173.52(7)	173.67(5)	170.61(9)	170.65(6)
E(1)–M(1)–P(2)	83.93(6)	100.33(7)	100.10(6)	85.10(8)	90.08(6)
E(2)–M(1)–P(1)	100.29(6)	93.05(7)	94.30(5)	99.48(8)	101.12(6)
E(2)–M(1)–P(2)	173.60(6)	178.53(9)	178.76(7)	173.53(8)	172.16(6)
P(1)–M(1)–P(2)	85.84(7)	85.71(8)	86.01(7)	85.9(1)	86.69(8)
E(2)–M(1)–E(1)–C(11)	−33.0(3)	−171.9(2)	−174.0(2)	9.8(4)	74.0(1)
E(1)–M(1)–E(2)–C(21)	179.9(3)	85.7(4)	86.8(2)	172.2(3)	−172.4(2)
M(1)–E(1)–C(11)–C(12)	90.5(7)	91.9(2)	93.9(5)	−96.5(9)	−6.7(1)
M(1)–E(1)–C(11)–S(11)	−91.8(4)	−100.7(5)	−100.5(4)	91.2(6)	173.5(2)
M(1)–E(2)–C(21)–C(22)	−92.4(8)	−37.4(1)	−43.3(6)	90.4(9)	−109.2(6)
M(1)–E(2)–C(21)–S(21)	99.5(5)	137.4(8)	134.8(4)	−102.8(6)	82.6(6)

one of the chalcogenolato ligands is almost coplanar with the $M(E_2)(P_2)$ plane in each complex. The orientation of the other ligand, however, depends on the E–M–E bond angle. The orientation of the aryl ring with respect to the M–E bond of the ligand also depends on the angle between the corresponding E–C bond and the $M(E_2)(P_2)$ plane.

The NMR spectroscopic and X-ray crystallographic information indicates the formation of only *cis*-[$M(EAr)_2$-(dppe)] complexes. The ^{77}Se or ^{125}Te resonances in **1**–**8** appear as second-order multiplets. Spectral simulation has yielded all relevant coupling constants. The trends in the ^{31}P, ^{77}Se, ^{125}Te, and ^{195}Pt chemical shifts expectedly depend on the nature of metal, chalcogen, and aryl group. We note that each trend can be considered independently of other factors.

Supplementary material

CCDC 631144, 631145, 631146, 631147, 631148, 631149, 631150, 631151, 631152 and 631153 contain the

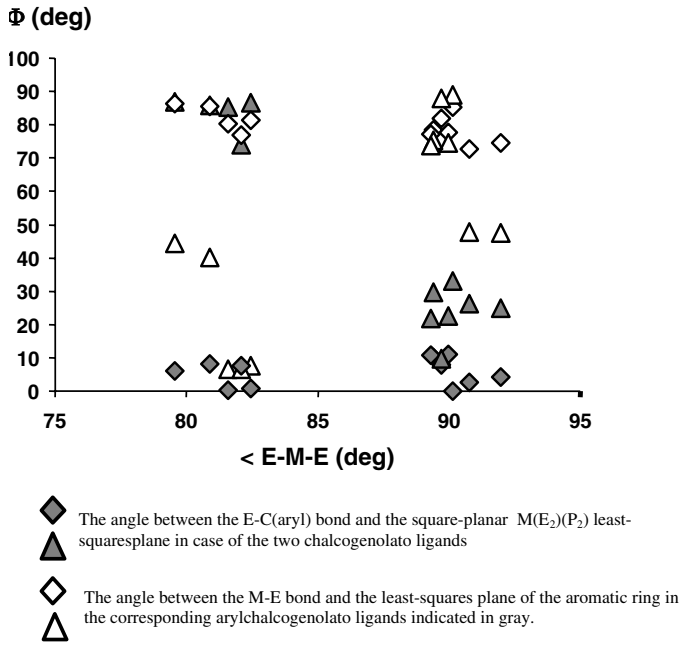

Fig. 7. The dependence of the angle between the least-squares planes containing the atoms M–E–C(aryl) (M = Pd, Pt; E = Se, Te; aryl = Ph, Th) and the square-planar coordination plane $M(E_2)(P_2)$ on the E–M–E bond angle in **1**–**8**. One E–C bond in each complex is approximately coplanar with the coordination plane (indicated with a gray square). The angle of the second E–C bond (indicated with a gray triangle) is more strongly dependent on the E–M–E bond angle. The open square and open triangle indicate the angle between the E–C bond and the aromatic rings. The open square defines the bond that is coplanar with coordination plane and the open triangle defines the E–C bond of the other chalcogenolato ligand.

supplementary crystallographic data for **1**–**8**, **3** · CH_3OH, and **7** · 1/2 CH_2Cl_2. These data can be obtained free of charge via http://www.ccdc.cam.ac.uk/conts/retrieving.html, or from the Cambridge Crystallographic Data Centre, 12 Union Road, Cambridge CB2 1EZ, UK; fax: (+44) 1223-336-033; or e-mail: deposit@ccdc.cam.ac.uk.

Acknowledgement

Financial support from Academy of Finland is gratefully acknowledged.

References

[1] V.P. Ananikov, M.A. Kabeshov, I.P. Beletskaya, G.G. Aleksandrov, I.L. Eremenko, J. Organomet. Chem. 687 (2003) 451.
[2] V.P. Ananikov, I.P. Beletskaya, G.G. Aleksandrov, I.L. Eremenko, Organometallics 22 (2003) 1414.
[3] V.P. Ananikov, I.P. Beletskaya, Doklady Chem. 389 (2003) 81.
[4] V.P. Ananikov, N.V. Orlov, I.P. Beletskaya, Russ. Chem. Bull. Int. Ed. 54 (2005) 576.
[5] V.P. Ananikov, I.P. Beletskaya, Org. Biomol. Chem. 2 (2004) 284.
[6] V.P. Ananikov, M.A. Kabeshov, I.P. Beletskaya, V.N. Khrustalev, M.Y. Antipin, Organometallics 24 (2005) 1275.
[7] R. Oilunkaniemi, R.S. Laitinen, M. Ahlgrén, J. Organomet. Chem. 587 (1999) 200.
[8] R. Oilunkaniemi, R.S. Laitinen, M. Ahlgrén, J. Organomet. Chem. 623 (2001) 168.
[9] R. Zanella, R. Ros, M. Graziani, Inorg. Chem. 12 (1973) 2736.
[10] I. Nakanishi, S. Tanaka, K. Matsumoto, S. Ooi, Acta Crystallogr. C50 (1994) 58.
[11] M.S. Hannu-Kuure, K. Paldán, R. Oilunkaniemi, R.S. Laitinen, M. Ahlgrén, J. Organomet. Chem. 667 (2003) 38.
[12] M.S. Hannu-Kuure, R. Oilunkaniemi, R.S. Laitinen, M. Ahlgrén, Acta Crystallogr. E60 (2004) m214.
[13] A. Wagner, M.S. Hannu-Kuure, R. Oilunkaniemi, R.S. Laitinen, Acta Crystallogr. E61 (2005) m2198.
[14] M.S. Hannu, R. Oilunkaniemi, R.S. Laitinen, M. Ahlgrén, Inorg. Chem. Commun. 3 (2000) 397.
[15] M.S. Hannu-Kuure, J. Komulainen, R. Oilunkaniemi, R.S. Laitinen, R. Suontamo, M. Ahlgrén, J. Organomet. Chem. 666 (2003) 111.
[16] R. Oilunkaniemi, R.S. Laitinen, M. Ahlgrén, J. Organomet. Chem. 595 (2000) 232.
[17] L.-Y. Chia, W.R. McWhinnie, J. Organomet. Chem. 148 (1978) 165.
[18] R. Oilunkaniemi, R.S. Laitinen, J. Pursiainen, M. Ahlgrén, Phosphorus, Sulfur, Silicon 136–138 (1998) 577.
[19] M.S. Hannu-Kuure, A. Wagner, T. Bajorek, R. Oilunkaniemi, R.S. Laitinen, M. Ahlgrén, Main Group Chem. 4 (2005) 49.
[20] N.V. Kirij, W. Tyrra, I. Pantenburg, D. Naumann, H. Scherer, D. Naumann, Y.L. Yagupolskii, J. Organomet. Chem. 691 (2006) 2679.
[21] (a) V.K. Jain, S. Kannan, E.R.T. Tiekink, J. Chem. Res. (S) (1994) 85;
(b) V.K. Jain, S. Kannan, E.R.T. Tiekink, J. Chem. Res. (M) (1994) 0501.
[22] S.K. Gupta, B.L. Khandelwal, Ind. J. Chem. 29A (1990) 977.
[23] C. Xu, J.W. Siria, G.K. Anderson, Inorg. Chim. Acta 206 (1993) 123.
[24] A. Singhal, V.K. Jain, B. Varghese, E.R.T. Tiekink, Inorg. Chim. Acta 285 (1999) 190.
[25] S. Dey, V.K. Jain, B. Varghese, J. Organomet. Chem. 623 (2001) 48.
[26] T. Appleton, M.A. Bennett, I.B. Tomkins, J. Chem. Soc., Dalton Trans. (1976) 439.
[27] D.P. Santry, H.P.A. Mercier, G.J. Schrobilgen, ISOTOPOMER A Multi-NMR Simulation Program, version 3.02NTF, Snowbird Software Inc., Hamilton, Ont., Canada, 2000.
[28] A. Altomare, G. Cascarano, C. Giacovazzo, A. Gualardi, J. Appl. Cryst. 26 (1993) 343.
[29] G.M. Sheldrick, SHELXL-97. Program for Crystal Structure Refinement, University of Göttingen, 1997.
[30] S. Dey, V.K. Jain, A. Knoedler, W. Klaim, S. Zalis, Eur. J. Inorg. Chem. (2001) 2965.
[31] S. Dey, V.K. Jain, J. Singh, V. Trehan, K.K. Bhasin, B. Varghese, Eur. J. Inorg. Chem. (2003) 744.
[32] S. Ford, C.P. Morley, M. Di Vaira, New J. Chem. 23 (1999) 811.
[33] S. Ford, C.P. Morley, M. Di Vaira, Inorg. Chem. 43 (2004) 7101.
[34] S. Kato, O. Niyomura, Y. Kawahara, T. Kanda, J. Chem. Soc., Dalton Trans. (1999) 1677.
[35] B. Khandelwal, K. Kundu, S.K. Gupta, Inorg. Chim. Acta 148 (1988) 255.
[36] H.C.E. McFarlene, W. McFarlene, J. Chem. Soc., Dalton Trans. (1973) 2416.
[37] T. Kemmitt, W. Levason, M. Webster, Inorg. Chem. 28 (1989) 692.
[38] R. Oilunkaniemi, J. Komulainen, R.S. Laitinen, M. Ahlgrén, J. Pursiainen, J. Organomet. Chem. 129 (1998) 521.
[39] Y. Kawahara, S. Kato, T. Kanda, T. Murai, K. Miki, J. Chem. Soc., Dalton Trans. (1996) 79.
[40] C.A. Grygon, W.C. Fultz, A.L. Rheingold, J.L. Burmeister, Inorg. Chim. Acta 144 (1988) 31.
[41] E.C. Alyea, G. Ferguson, S. Kannan, Polyhedron 17 (1998) 2231.
[42] V.K. Jain, S. Kannan, R.J. Butcher, J.P. Jasinski, J. Chem. Soc., Dalton Trans. (1993) 1509.

[43] L.B. Kumbhare, V.K. Jain, B. Varghese, Inorg. Chim. Acta 359 (2006) 409.
[44] S. Dey, V.K. Jain, A. Knödler, A. Klein, W. Kaim, S. Záliš, Inorg. Chem. 41 (2002) 2864.
[45] D.M. Giolando, T.B. Rauchfuss, A.L. Rheingold, Inorg. Chem. 26 (1987) 1636.
[46] P.J. Bonasia, J. Arnold, J. Organomet. Chem. 449 (1993) 147.
[47] C. Nishitani, T. Shizuka, K. Matsumoto, S. Okeya, H. Kimoto, Inorg. Chem. Commun. 1 (1998) 325.
[48] R. Oilunkaniemi, R.S. Laitinen, M. Ahlgrén, Z. Naturforsch. 55b (2000) 361, and references therein.